

Role of Alloying Elements and Carbides in the Chlorine-Induced Corrosion of Steels and Alloys

Hans Jürgen Grabke, Michael Spiegel, Armin Zahs*

*Max-Planck-Institut für Eisenforschung
Max-Planck-Straße 1, D-40237 Düsseldorf, Germany*

Received: September 2, 2002; Revised: September 4, 2002

The high temperature corrosion of steels and Ni-base alloys in oxidizing and chloridizing environments is of practical interest in relation to problems in waste incineration plants and power plants using Cl containing fuels. The behaviour of the most important alloying elements Fe, Cr, Ni, Mo, Mn, Si, Al upon corrosion in an oxidizing and chloridizing atmosphere was elucidated: the reactions and kinetics can be largely understood on the base of thermodynamic data, i.e. free energy of chloride formation, vapor pressure of the chlorides and oxygen pressure p_{O_2} needed for the conversion chlorides \rightarrow oxides.

The mechanism is described by 'active oxidation', comprising inward penetration of chlorine into the scale, formation of chlorides at the oxide/metal interface, evaporation of the chlorides and conversion of the evaporating chlorides into oxides, which occurs in more or less distance from the surface (depending on p_{O_2}). This process leads to loose, fragile, multilayered oxides which are unprotective (therefore: active oxidation). Fe and Cr are rapidly transferred into such scale, Ni and Mo are relatively resistant.

In many cases, the grain boundaries of the materials are strongly attacked, this is due to a susceptibility of chromium carbides to chloridation. In contrast the carbides Mo_2C , TiC and NbC are less attacked than the matrix.

Alloys on the basis Fe-Cr-Si proved to be rather resistant, and the alloying elements Ni and Mo clearly retard the attack in an oxidizing and chloridizing environment.

Keywords: chloridation, active oxidation, model alloys, alloying elements, carbides

1. Introduction: Reactions and mechanisms

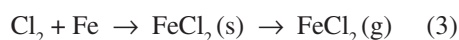
Oxidation can be considerably accelerated in presence of chlorine, hydrogen chloride and chlorides, this is a problem in waste incineration plants and power plants fired with chloride containing coal. Chlorine formation occurs from HCl through catalysis by oxide scales



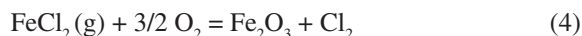
or from chlorides by reaction with oxides such as Fe_2O_3



Chlorine can somehow diffuse through oxide scales rapidly and reacts at the interface oxide/metal to chlorides of Fe, Ni and the other alloying elements, e.g.



$FeCl_2(s)$ has a vapor pressure at 500 °C of 5×10^{-4} bar, and will evaporate steadily. The $FeCl_2(g)$ passes through cracks and pores of the scale outwards, and when reaching regions with sufficient oxygen pressure it is oxidized according to



The oxides growing from the vapor phase near or at the scale surface are very fragile and not protective. The chlorine from reaction (4) may enter the atmosphere but mostly will reenter the scale and continue its catalytic action in the reaction sequence (2), (3) and (4). This mechanism is also called 'active oxidation' (Fig. 1) since it does not lead to a

*e-mail: grabke@mpie.de

Presented at the International Symposium on High Temperature Corrosion in Energy Related Systems, Angra dos Reis - RJ, September 2002.

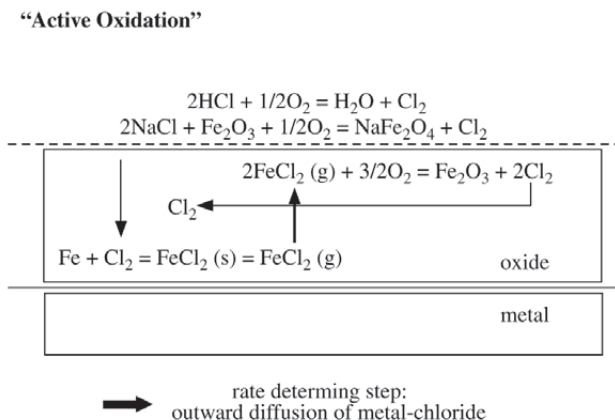


Figure 1. Schematics of the reaction circuit in active oxidation of iron and steels.

dense protective scale (passivation) but to an active, accelerated corrosion¹⁻².

The chlorine plays a catalysing role and often is not easily found in failure case studies³. In a detailed study of effects of chlorides on the oxidation of a low alloy steel it was shown that the outward diffusion of the gaseous $\text{FeCl}_2(\text{g})$ is rate determining for this corrosion process⁴⁻⁵. ‘Active oxidation’ also takes place on high alloy steels⁵⁻⁶ under formation of voluminous non protective scales. These steels also show a typical grain boundary attack under oxidizing and chloridizing conditions, i.e. holes and internal oxides are formed at grain boundaries where chromium carbides had been before^{3,7}.

After these studies on steels, it was of fundamental interest how the other alloying elements in steels behave in the ‘active oxidation’ process. Furthermore the reaction of carbides was of interest and both reactions of alloying elements and of carbides in model alloys were studied fundamentally in an oxidizing and chloridizing atmosphere⁷⁻¹⁰.

2. Experimental

The experiments were carried out in the temperature range 400 - 700 °C, exposure tests in flowing N_2 -5% O_2 -500-1500 vppm HCl and thermogravimetric tests in He-5% O_2 -500-1500 vppm HCl. The pure elements Fe, Cr and Ni were tested and model alloys Fe-15% Cr - with either 10% Mn, 10% Mo, 5% Ti, 5% Al or 5% Si and Fe-35% Cr. In some of these materials carbides were generated by addition of 0.3% carbon and an appropriate heat treatment. Furthermore some commercial alloys were studied: Alloys 800, 825, 625 and 625 Si⁹⁻¹⁰.

3. Results

3.1. Pure metals: Fe, Cr and Ni

Thermogravimetric studies on the corrosion of Fe in He-5% O_2 -500 vppm HCl showed the most severe corrosion of the three metals. At 400 °C an outer 2-3 μm thick oxide layer and a 6 - 10 μm thick $\text{FeCl}_2(\text{s})$ layer was observed after 168 h. At 500 °C the outer oxide scale is 10 - 15 μm thick and its crystalline, filigrane morphology indicates its formation from the gas phase according to reaction (4). Beneath this layer are grown oxides and chloride at the oxide/metal interface. Most striking is the appearance of the corrosion products after 168 h at 600 °C - the oxide is formed like a dome over the sample. Its shape corresponds to the stagnant diffusion boundary layer through which $\text{FeCl}_2(\text{g})$ diffuses into the region where $p\text{O}_2$ is high enough for the conversion $\text{FeCl}_2(\text{g}) \rightarrow \text{Fe}_3\text{O}_4$ and Fe_2O_3 . Fe_3O_4 was found at the interior and Fe_2O_3 at the outer surface of the oxide bubble, $\text{FeCl}_2(\text{s})$ on the surface of the metal phase.

On chromium at 400 and 500 °C thin Cr_2O_3 layers were formed and chlorides were detected only locally. At 600 and 700 °C the scales frequently cracked and spalled as seen in the kinetics. This leads to a multilayered oxide scale see Fig. 2, beneath this scale a layer was detected consisting of a mixture of oxide and chloride.

On the nickel sample at 400 °C simultaneous formation of oxides and chlorides occurred. At 500 °C considerable evaporation of NiCl_2 leads to parabolic kinetics. Also at 600 and 700 °C NiCl_2 evaporation prevails and the evaporating chloride is not oxidized near the sample but carried away by the gas flow.

3.2. Binary alloys Fe-15% Cr and Fe-35% Cr

The corrosion of the binary Fe-Cr alloys is strongly dependent on the temperature and less on the HCl content (500 or 1500 vppm) of the atmosphere.

At 400 and 500 °C after 168 h, the mass gains by corrosion are low, protective Cr_2O_3 -scales are formed and only locally destroyed by outgrowth of $(\text{Fe}, \text{Cr})\text{Cl}_2$ crystals. At 500 °C the Fe-15% Cr alloy already shows indications of active oxidation and enhanced attack, compared to Fe-35% Cr.

At 600 °C the attack on both alloys is very severe, mass gains are higher than for all other alloys studied, even higher than on iron. The adverse features of both, Fe and Cr, in the ‘active oxidation’ are combined: poorly adherent multilayers of oxides are formed due to repeated cracking and spalling. The layers are Fe-rich at their outside (Fe_2O_3 , $(\text{Fe}, \text{Cr})_3\text{O}_4$) and Cr-rich at their inside surface (FeCr_2O_4 , Cr_2O_3). At the oxide/metal interface the mixed chloride $(\text{Fe}, \text{Cr})\text{Cl}_2$ was found, and the grain boundaries of the alloys were attacked.

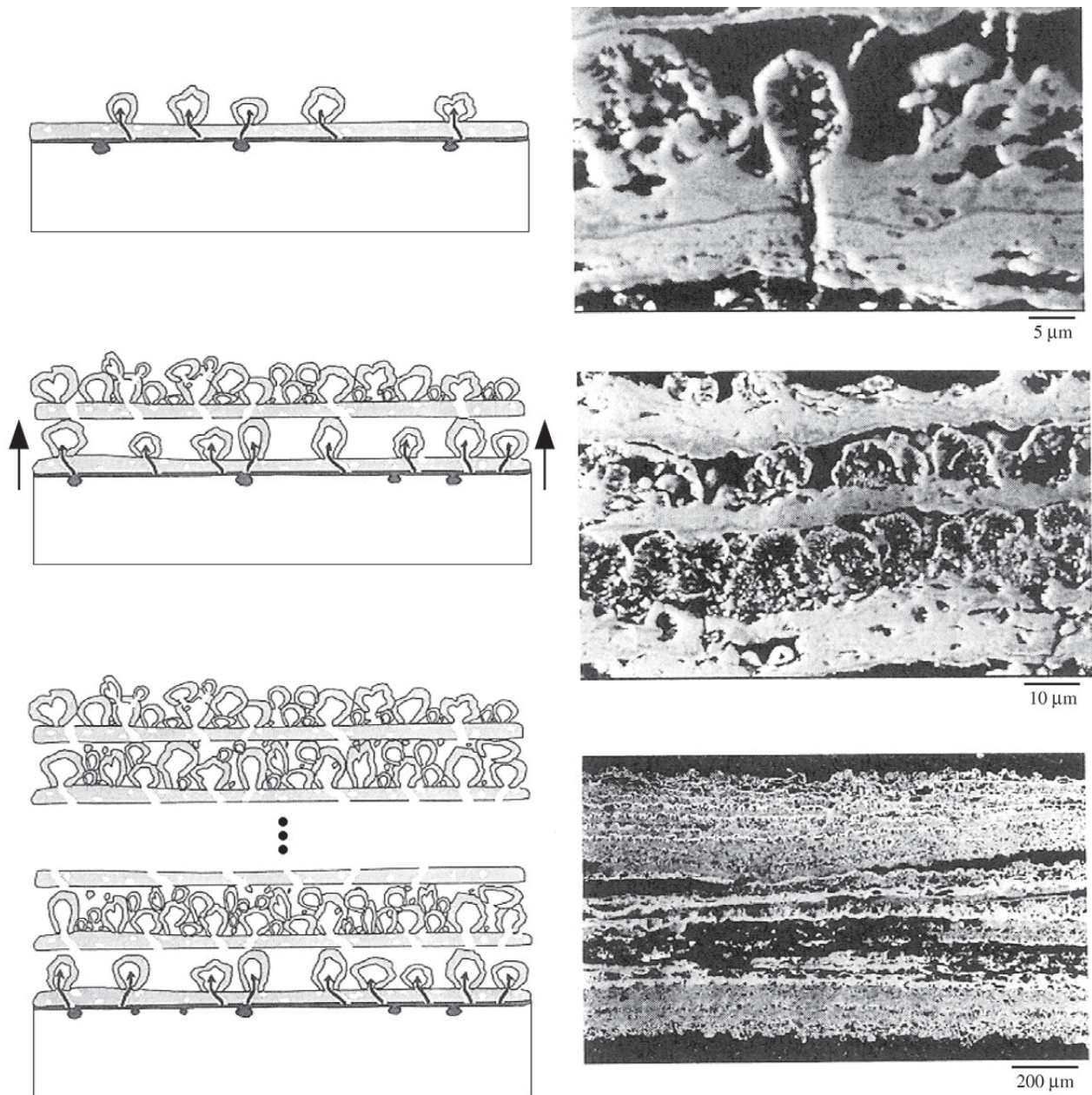


Figure 2. Growth of multilayered oxide scales by active oxidation of Cr, Fe-15% Cr, Fe-35% Cr, Fe-15% Cr-5% Ti etc.; a) schematic model; b) scale grown on Fe-15% Cr-5% Ti after 168 h in N_2 -5% O_2 -500 vppm HCl at 600 °C (in different magnifications).

It was shown that the evaporating chlorides were nearly completely converted to oxides, $FeCl_2$ in the outer part of each layer and $CrCl_2$ in the inner part. The repeated fracture and spalling of the outermost growing layer leads to formation of the special structure, with oxide bubbles and layers, see Fig. 2.

3.3. Ternary alloys Fe-15% Cr-M

Results are reported of exposures in N_2 -5% O_2 -500-1500 vppm HCl, mainly at 600 °C for 168 h, see Fig. 3.

Fe-15% Cr-5% Ti corrodes as severely as the binary Fe-Cr alloys. The morphology of the scale indicates that

the mechanism of the scale growth is the same: formation of a multilayer by active oxidation, repeated cracking and spalling of the layers and formation of oxide bubbles over cracks. The metal phase contains intermetallic compounds $\text{Cr}_6\text{Fe}_{18}\text{Ti}_5$ as precipitates and they are preferentially attacked, due to the highly negative free energies of Ti-chlorides formation.

Fe-15% Cr-10% Mn is less corroded than the Fe-Cr alloys. A voluminous scale is formed consisting of Fe_2O_3 and Mn_2O_3 at its outside and Cr_2O_3 at the inside, the morphology similar as in the case of Fe, like large bubbles. In the cavity beneath, the oxygen pressure obviously is low, since its bottom is covered with chlorides, (Mn, Fe, Cr) Cl_2 crystals for the condition 500 vppm HCl and a CrCl_2 -layer at 1500 vppm HCl. The latter layer obviously hems the corrosion, which is less at the higher HCl content.

Fe-15% Cr-10% Mo shows improved corrosion resistance compared to the binary Fe-Cr alloys. Beneath the Fe- and Cr-oxides in the scale the metal phase is depleted of Fe and Cr and enriched in Mo. Obviously selective corrosion of Fe and Cr has occurred and the Mo reacts much slower, because the free energy of Mo-chlorides formation is less than the values for FeCl_2 and CrCl_2 formation. This zone of about 5 μm thickness is porous and allows the access of the corrosion gases to the uncorroded metal phase, but its presence obviously retards the attack.

Fe-15% Cr-5% Al proved to be very corrosion-resistant in the exposure tests with 500 and 1500 vppm HCl. At the relatively low gas flow velocities a protective scale of $\gamma\text{-Al}_2\text{O}_3$ was formed and only locally outgrowth of Fe and Cr-oxides occurred. This observation already indicates the corrosion resistance may not be reliable. In fact, the thermogravimetric experiments at higher flow velocities showed strong active oxidation under formation of a multilayered porous scale. Probably at the higher flow velocities the evaporating AlCl_3 is transported away before conversion to a protective oxide scale. Also differences were observed after different surface finish, a ground specimen corroded much faster than a polished one.

Most corrosion resistant was the **Fe-15% Cr-5% Si** alloy, also at high gas flow velocities. The protection is effected by a thin Cr_2O_3 -rich oxide scale, only locally some iron oxides have grown by active oxidation. An internal layer of SiO_2 was not detected, but probably initial formation of such layer and enhanced Cr-diffusion in the alloy have led to formation of the protective scale. Fe-Cr-Si alloys have been tested thoroughly under simulated waste incineration conditions, and they may be used as coatings for effectively improving corrosion resistance¹¹⁻¹².

3.4. Commercial alloys containing nickel

To study the role of nickel, the commercial alloys Alloy 800, i.e. Fe-30.3 Ni-20.3 Cr and Alloy 600 Ni - 16 Cr-8.3 Fe

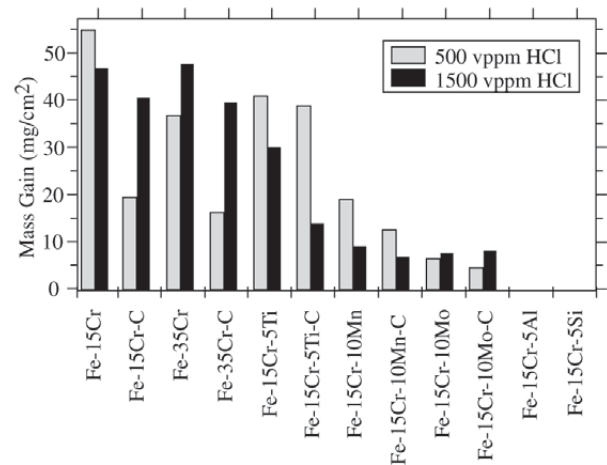


Figure 3. Mass changes of the model alloys after 168 h corrosion in N_2 -5% O_2 -500 or 1500 vppm HCl.

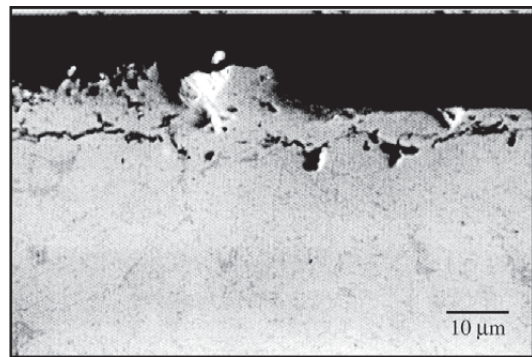
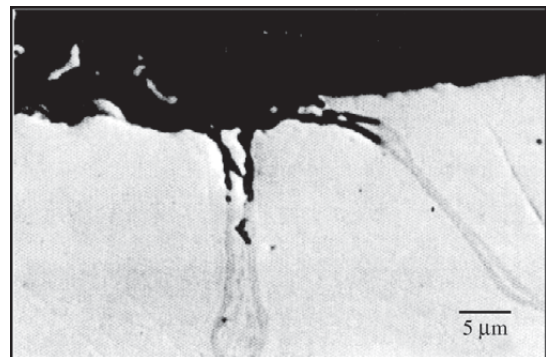
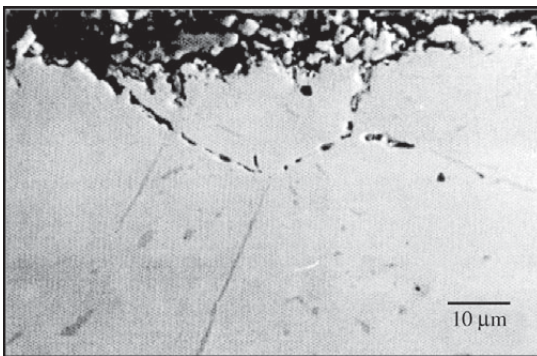
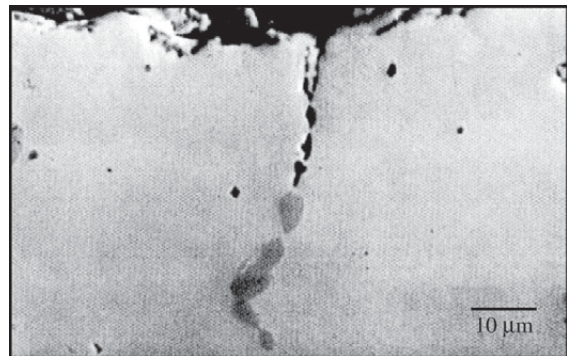
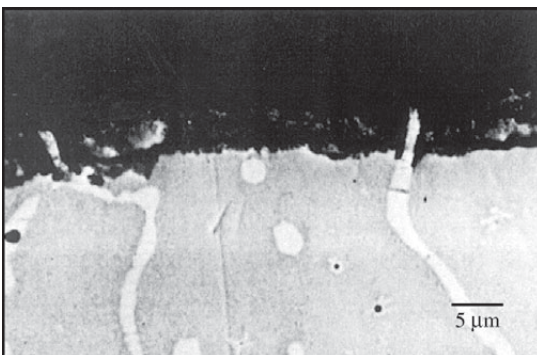
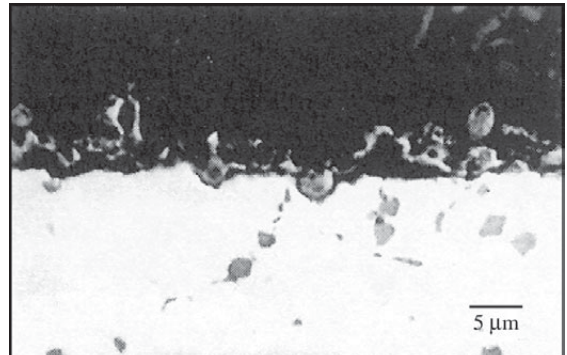
were tested at 600 °C in the oxidizing-chloridizing atmosphere. These alloys behave relatively inert compared to the Cr-steels. The mass increase after 168 h is about 1.75 mg/cm^2 for Alloy 800 and 0.5 mg/cm^2 for Alloy 600 in both atmospheres with 500 or 1500 vppm HCl (compared values between 5-50 mg/cm^2 , see Fig. 3). As in the case of Mo the attack on Ni is less than on Fe and Cr, because the free energy of NiCl_2 - formation is much less negative than for FeCl_2 and CrCl_2 . In the alloys 800 and 600 the selective corrosion of Fe and Cr leads to a porous, sponge like structure of the outer zone of the metal phase. The evaporating chlorides FeCl_2 and CrCl_2 are oxidized above the oxide/metal interface and form a multilayered scale, as in the case of the Fe-Cr alloys, consisting of Fe_2O_3 and (Fe, Ni) Cr_2O_4 . The morphology of the scale on Alloy 800 is characterized by voluminous oxide bubbles and on Alloy 600 by many thin layers.

The attack by the oxidizing-chloridizing is even more suppressed by additional alloying with Mo, this was shown for Alloy 625, i.e. Ni-22.2 Cr-9.2 Mo-4.6 Fe-3.4 Nb, and for Alloy 625Si, i.e. Ni-20.8 Cr-9.5 Mo-3.2 Fe-1.5 Si, for which the corrosion resistance was best.

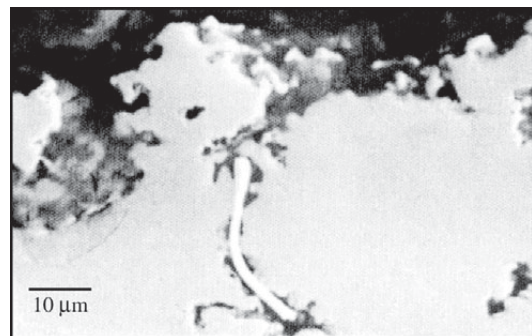
3.5. Alloys with carbide precipitates

Well-defined carbides were obtained in ternary Fe-Cr-C and quaternary Fe-Cr-M-C alloys by appropriate heat treatments⁷. These alloys were tested as the others in the oxidizing-chloridizing environment at 600 °C for 168 h.

M_{23}C_6 carbides in Fe-15% Cr-0.8% C, Fe-35% Cr-0.3% C and Fe-20% Cr-12% Ni-0.3% C were strongly attacked beginning from the sample surface. The preferential attack of the carbides leads to holes in the metal matrix, see Fig. 4a-4c, thus the components must have left the speci-

a) $M_{23}C_6$ in Fe-15Cr-Cb) $M_{23}C_6$ in Fe-35Cr-0.8Cc) $M_{23}C_6$ in Fe-20Cr-12Ni-Cd) M_7C_3 in Fe-20Cr-33Ni-Ce) M_6C in Fe-15Cr-10Mo-C

f) TiC in Fe-15Cr-15Ti-C



g) NbC in Fe-18Cr-10Ni-0.8Nb-0.1C

Figure 4. Metallographic cross sections of model alloys with well-defined carbide precipitates after 168h corrosion in N_2-O_2-HCl at 600 °C. a-d) the chromium carbides $M_{23}C_6$ and M_7C_3 are attacked selectively; e-g) Mo-rich carbide M_6C , TiC and NbC are clearly more corrosion resistant than the metal matrix.

mens as gaseous reaction products. this is possible by the reaction which has a considerably negative free energy.



Also M_7C_3 obtained by heat treatment of Fe-20% Cr-33% Ni-0.5% C is attacked preferentially and the corrosion leaves cavities along the grain boundaries (Fig. 4d). So the chromium carbides M_{23}C_6 and M_7C_3 are weak components in the corrosion of alloys in oxidizing-chloridizing conditions. Often failure cases have been reported where the grain boundary attack in such environment is due to the grain boundary carbides in high temperature steels and alloys.

In contrast other carbides such as Mo_6C , TiC and NbC prepared in Fe-15% Cr-10% Mo-0.3% C, Fe-15% Cr-5% Ti-0.3% C and Fe-18% Cr-10% Ni-0.8% Nb-0.1% C, behaved better corrosion resistant than the matrix. These carbides remain nearly unattacked even after the surrounding metal matrix has corroded, see Fig. 4e-g. This observation was surprising since also for these carbides the reactions leading to volatile chlorides and CO have negative free energies. So the reason for the stability of TiC, NbC and Mo_6C in the oxidizing-chloridizing environment is not clear as yet.

4. Discussion

The corrosion behaviour of the alloying elements in oxidizing-chloridizing environments can be discussed and explained largely by thermodynamic data (see Fig. 5):

- The *Gibbs' free energy of the reaction metal + chlorine @ metal chloride*. The more negative this value the faster is the reaction with this element in the metal matrix and the corrosion attack occurs according to the sequence $\text{Mn} > \text{Cr} > \text{Fe} > \text{Ni} > \text{Mo}$.
- The *oxygen pressure for the conversion of the evaporating chlorides into oxides*, e.g. reaction (4). The lower this oxygen pressure, the smaller is the distance from the metal surface at which the oxide is formed. Therefore the oxide layers are Fe-rich at their outside and Cr-rich at their inside, and the Ni- and Mo-chloride are transported away to a great part unoxidized by the gas flow.
- The *vapor pressures of the chlorides*, they also play a role for the destiny of the corrosion products, evaporation or oxidation.

5. Conclusions

The corrosion of metals and alloys in oxidizing-chloridizing environments occurs by 'active oxidation'⁴⁻⁶, i.e. the reaction steps: i) formation of Cl_2 from HCl or chlorides in and on the oxide scale, ii) penetration of Cl_2 into the scale and reaction to metal chlorides at the metal phase, (iii) outward diffusion of metal chlorides through the scale

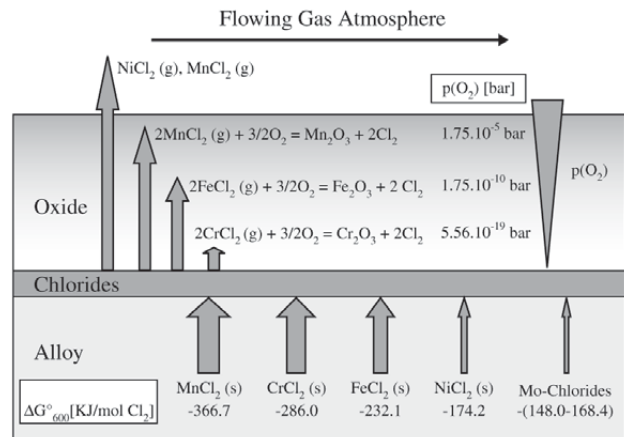


Figure 5. Schematic of thermodynamics and reactions in the corrosion of the alloying elements Mn, Cr, Fe, Ni and Mo in a flowing oxidizing and chloridizing atmosphere.

and (iv) oxidation of the chlorides to crystalline, porous oxides, where a region with a sufficient p_{O_2} is reached in or over the scale. The Cl_2 reenters the scale, so the active oxidation is a circuit catalysed by chlorine, leading to an unprotective oxide scale.

The reaction of Cl_2 with the alloying elements⁸⁻¹⁰ is the faster the more negative the free energy of chloride formations is, Cr, Fe and Mn are attacked strongly, whereas Ni and Mo react slowly and behave rather inert. From Ni and/or Mo rich alloys the other alloying elements are reacted selectively and a porous Ni and Mo rich metal layer remains. Thus Ni and Mo are favourable for the corrosion resistance of alloys in oxidizing-chloridizing environments.

On Cr, Fe-Cr and Fe-Cr-M alloys ($\text{M} = \text{Ti}, \text{Mn}$) friable unprotective scales are formed. Layers of Cr_2O_3 , spinels and Fe_2O_3 result from the evaporation and oxidation of FeCl_2 and CrCl_2 , oxide bubbles arise where such layers are cracking and repeated spalling and cracking leads to a multilayered scale. Si and Al as alloying elements M can significantly retard this corrosion process. Fe-Cr-Si alloys are recommended as protective coatings in oxidizing-chloridizing environments¹¹⁻¹².

Chromium carbides M_7C_3 and M_{23}C_6 are strongly attacked in oxidizing-chloridizing environments, this leads to grain boundary corrosion of alloys with such grain boundary carbides, starting from the surface⁷⁻¹⁰. Since gaseous reaction products, CrCl_2 and CO, are formed, holes are left in the metal matrix and internal oxidation follows. Other carbides such as Mo_6C , TiC and NbC are more corrosion resistant than the alloy matrix and stay uncorroded. Accordingly, presence or formation of chromium carbides should be avoided in alloys applied in oxidizing-chloridizing environments.

References

1. McNallan, M.J.; Liang, W.W.; Kim, S.H.; Kong, C.T. in "High Temperature Corrosion", R.A. Rapp ed., NACE, 136, 1983.
2. Lee, Y.Y.; McNallan, M.J. *Metallurg. Trans 18A*, 1099 (1987).
3. Grabke, H.J.; Müller, E. *Werkstoffe u. Korr. 41*, 226 (1990).
4. Reese, E.; Grabke, H.J. *Werkstoffe u. Kor. 44*, 41 (1993).
5. Grabke, H.J.; Reese, E.; Spiegel, M. *Corros. Sci 37*, 1023 (1995).
6. Reese, E.; Grabke, H.J.; *Werkstoffe u. Korr. 43*, 547 (1992).
7. Berztiss, D.; Zahs, A.; Schneider, A.; Spiegel, M.; Viefhaus, H.; Grabke, H.J. *Z. Metallkd. 90 1* (1991).
8. Zahs, A.; Spiegel, M.; Grabke, H.J. *Materials & Corr.* 50, 561 (1999).
9. Zahs, A. *Chlorinduzierte Hochtemperaturkorrosion in oxidierenden Atmosphären*. Fortschritt-Berichte VDI, Reihe 5, Nr. 551, VDI Verlag GmbH, Düsseldorf, (Dr.-Thesis) 1999.
10. Zahs, A.; Spiegel, M.; Grabke, H.J. *Corros. Sci. 42*, 1093 (2000).
11. Schroer, C. *Entwicklung neuer Werkstoffe zur Verlängerung der Standzeit von Wärmetauschern in Müllverbrennungsanlagen*. Shaker Verlag Aachen (Dr. Thesis) 2001.
12. Schroer, C.; Spiegel, M.; Grabke, H.J.; Sauthoff, G. *Europäisches Patent EP 0933 443 B1*, Use of steel powder based on Fe-Cr-Si for corrosion resistant coating, granted and published 03.04.2002.